RSC Advances

PAPER

View Article Online
View Journal | View Issue

Cite this: *RSC Adv.*, 2015, **5**, 95247

Simultaneous adsorption of Cd^{2+} and reactive dye on mesoporous nanocarbons†

Beatriz Acevedo and Carmen Barriocanal*

Received 15th October 2015
Accepted 26th October 2015

DOI: 10.1039/c5ra21493a

www.rsc.org/advances

High-surface-area mesoporous MgO-templated nanocarbons made with reinforcing fibres from scrap tyres and a bituminous waste as carbon precursors were employed for the simultaneous adsorption of Cd^{2+} and reactive Cibacron Brilliant Yellow 3G-P dye. A commercial activated carbon (AC) Darco KB-WJ was also used for comparison purposes. The effect of the pH of the solution was studied to establish whether acidic pH favours the adsorption of reactive dye and alkaline pH improves the removal of Cd^{2+}. Because the surface chemistry of the three adsorbents was similar, the focus in this study was directed towards their textural characteristics. It was found that the larger the S_{BET}, the greater the amount of dye removal. The adsorption isotherms corresponding to the commercial AC fitted to the Langmuir–Freundlich model, whereas in the case of the nanocarbons the Langmuir model provided the best fit. The results obtained show that Cd^{2+} is successfully adsorbed in the presence of the dye due to the ion exchange between the Na^{+} from the dye and the Cd^{2+}. It was also found that a high total and mesopore volume, and a high S_{BET} played a determinant role in the simultaneous adsorption.

1. Introduction

The pollution from textile wastewaters is mainly due to the large amount of suspended solids (SS), high chemical oxygen (COD) and biochemical oxygen demand (BOD), in conjunction with other factors such as heat, colour, acidity, basicity and toxic metals. Most pollutants, except for colour, can be reduced by conventional sewage treatment works.[1] Dyes are difficult to eliminate due to their complex structure and synthetic origin which make them more stable.[2] Moreover, their presence reduces aquatic diversity because they block the passage of light through the water, thereby preventing the photosynthesis of aquatic flora.[1,3] There is a large variety of dyes (acid, basic, reactive, direct, dispersive, sulphur and metallic dyes) that come under the category of cationic, non-ionic or anionic. Water soluble reactive and acid dyes are the most problematic since neither conventional biological treatment processes nor physicochemical coagulation/flocculation methods are able to remove them.[1,4]

Metals are present in dyes because in some cases they are used as catalysts during their manufacture and may persist as impurities or exist in dye molecules, where they form an integral part of their structure. Another serious problem in decontamination technology is the presence of heavy metals and ions in textile industrial effluents. Due to their toxicity, these pollutants are considered to be very dangerous to human health and the environment. Heavy metals commonly found in textile wastewater are Cr^{6+}, Cu^{2+}, Cd^{2+}, Pb^{2+}, Ni^{2+}, Zn^{2+}.[5–7] Cadmium is one of these very toxic elements[8,9] accumulating in humans and competing with several life-essential metals like calcium, zinc and copper.[8] The most common use of cadmium is as an anti-corrosion protective coating for metals.[10]

Adsorption is considered to be an effective and relatively cheap process for removing dyes and has found a large number of applications. Many different types of adsorbents have proved to be effective in removing certain colours from aqueous effluents. The sorbents most commonly used to treat these effluents are activated carbons. However these are costly and their pore distribution cannot be controlled. To reduce the cost, "non-conventional" sorbents from various wastes have been prepared.[11–14]

Microporous and mesoporous carbons prepared by the template method with zeolite and silica as template allow materials with a homogeneous pore size and an optimum morphology to be obtained. The main problem with this method is the need to use corrosive acids. However these can be avoided by employing organic templates.[15] An alternative method to obtain adsorbents is to prepare mesoporous nanocarbons with MgO as template. This new template synthesis procedure is used to prepare porous carbons with a controlled structure from thermoplastic carbon precursors without the need for any stabilization and activation process.[16] In this case, an MgO precursor is essential, examples of which are magnesium citrate, magnesium acetate, magnesium gluconate, magnesium hydroxyl-carbonate or MgO itself.[15,17,18]

Instituto Nacional del Carbón, INCAR-CSIC, Apartado 73, 33080 Oviedo, Spain. E-mail: carmenbr@incar.csic.es; Fax: +34 985 29 76 62; Tel: +34 985 11 90 90

† Electronic supplementary information (ESI) available. See DOI: 10.1039/c5ra21493a

Reinforcing fibre from tyre waste could be an ideal carbon precursor. Scrap tyres are converted in tyre recycling plants into tyre crumbs, reinforcing fibre and steel.[19] Tyre crumbs have multiple applications but no use has yet been found for the reinforcing fibre which is obtained during the process of mechanical grinding of tyres after the metallic parts and the rubber have been removed. These wastes comprise a very heterogeneous material made up of a mixture of a fluff with thermoplastic properties, fine rubber and pieces of cord with rubber adhered to them.

The present study deals with the simultaneous adsorption of two contaminants present in the wastewater of textile industries, a reactive dye *i.e.* Cibacron Brilliant Yellow 3G-P and a heavy metal ion (Cd^{2+}), by means of MgO-templated nanocarbons obtained from reinforcing fibre. Thus a highly effective way to recycle waste has been found by making use of the waste itself to fabricate adsorbents. The primary aim of the present work was to study the effect of the interaction of the reactive dye and a heavy metal ion on adsorption and to ascertain the influence of the pore size distribution on the process. For comparison purposes a commercial activated carbon specifically prepared for the decolorization of effluents has been employed.

2. Materials and methods

2.1. Materials

The adsorbates used were reactive Cibacron Brilliant Yellow 3G-P, a commercial dye (CBY) (C.I. reactive yellow 2, $C_{25}H_{15}Cl_3N_9Na_3O_{10}S_3$, Fig. 1) and Cd^{2+} in the form of Cl_2Cd. Both of these adsorbates were acquired from Sigma-Aldrich. Distilled water was used to prepare the desired concentration of the Cd^{2+}, dye and dye + Cd^{2+} solutions. An UV/Vis absorption spectrophotometer UV-2450 Shimadzu was employed to measure the concentration of dye at $\lambda_{max} = 404$ nm and an ICP-MS 7700x Agilent was the instrument chosen to measure the Cd^{2+} concentration. Each measurement was repeated three times.

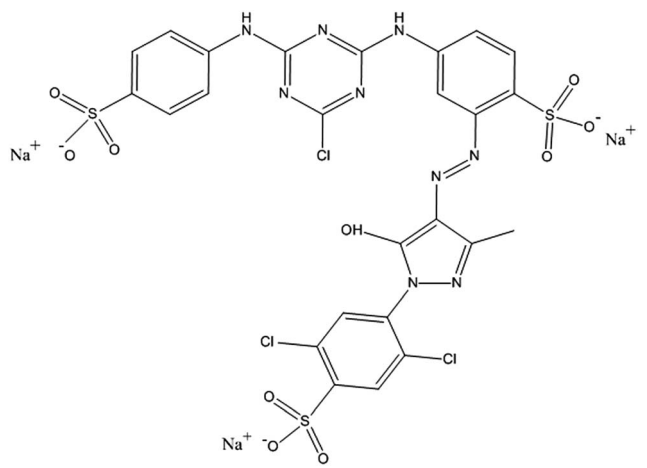

Fig. 1 Molecular structure of Cibacron Brilliant Yellow 3G-P dye. Molecular weight = 872.97 g mol^{-1}.

The adsorbents employed were MgO-templated nanocarbons prepared from the pyrolysis of a blend of reinforcing fibre from waste tyre, bituminous waste material and magnesium citrate in a rotary oven at a flow rate of 100 ml min^{-1} of N_2 and a heating rate of 5 °C min^{-1} up to 950 °C; two procedures were used: (i) powder mixing (sample C3BRFBWM_PM) where the mixture was heated in air up to the melting temperature and afterwards the mixture was pulverized in an agate mortar and carbonized. (ii) A solution mixing procedure (sample C3BRFBWM_SM) where the precursor was imbibed in a solution of Mg citrate and left to dry, the bituminous material being added once the fibre was dry. After carbonization, the MgO particles were removed by washing the carbons with 15 M HCl. The preparation procedure and the characteristics of these materials have been described in detail in a previous paper.[16] The textural properties of the nanocarbons were studied by means of N_2 adsorption at 77 K on a Micromeritics ASAP 2420 apparatus. The software package provided with the equipment was used to determine the textural parameters. The point of zero charge (pH_{PZC}) was determined according to the procedure described by Moreno-Castilla *et al.*[20] Briefly, 0.25 g of carbon was mixed with 10 ml of CO_2-free distilled water. The slurry was kept in a plastic bottle and shaken on an orbital shaker for 48 h. The final pH of the slurry was taken as the pH_{PZC} of the solid.

A commercial mesoporous AC *i.e.* Darco KB-WJ (AC Darco) obtained from Sigma-Aldrich especially designed for the adsorption of dyes from effluents was also used for comparison purposes.

2.2. SEM-EDX

The surface topography of the nanocarbons before and after adsorption was studied on a FEI QUANTA FEG 650 scanning electron microscope. Secondary electrons (SE) allowed the surface topography to be observed to within a lateral resolution of a few nanometers, whereas images produced by means of elastically backscattered electrons (BSE) provided an elemental contrast. Furthermore, characteristic X-ray detection allowed the atomic concentration to be determined at micrometer scale (energy-dispersive X-ray spectroscopy, EDX).

2.3. Batch adsorption experiments

The activated carbon samples were finely ground to a size smaller than 63 μm in order to avoid mass transfer limitations since the rate of adsorption and the time to reach equilibrium depend largely on the particle size of the adsorbent. The time necessary to achieve equilibrium was 72 h for adsorption of the dye, and 20 h for adsorption of the binary CBY–Cd^{2+} mixture in all the samples, as determined by preliminary adsorption tests. Preliminary tests were also carried out in order to obtain an initial dye concentration that would allow the study of the removal of the dye by the carbon materials. Equilibrium adsorption isotherms of the dye and Cd^{2+} in the different samples were performed at pH 7 by means of the following procedure: 50 ml of the CBY or CBY–Cd^{2+} solutions in different initial concentrations were mixed with 50 mg of adsorbent in closed 100 ml vessels. The initial concentrations ranged from 36

to 900 mg l^{-1} of reactive Cibacron Brilliant Yellow 3G-P dye and from 2.40 to 60 mg l^{-1} of Cd^{2+}. The vessels were wrapped up in aluminium foil to prevent the degradation of the dye by the action of light, and then placed in a shaker at room temperature until equilibrium was reached. Before the adsorption experiments, the initial pH was adjusted to pH 7 using either HCl 0.1 M or NH_4OH 0.1 M.

To study the influence of pH on the adsorption behaviour, the initial pH was increased from 2 to 12 in the case of the dye solution ($C_{o,dye}$ = 900 mg l^{-1}) and from 2 to 8 in the dye–Cd^{2+} solution ($C_{o,dye}$ = 900 mg l^{-1} and $C_{o,Cd^{2+}}$ = 60 mg l^{-1}) using HCl and NH_4OH.

The dye and heavy metal ($q_{e,i}$, mg g^{-1}) adsorption capacities of all the adsorbents were calculated by performing a mass balance (expressed by eqn (1)) where $C_{o,i}$ and $C_{e,i}$ are the initial and equilibrium concentrations (mg l^{-1}) of the dye or Cd^{2+} in solution, V is the volume (l) of the adsorbate solution used for the adsorption experiments and m is the amount of adsorbent (g), respectively.

$$q_{e,i} = \frac{(C_{o,i} - C_{e,i})V}{m} \quad (1)$$

3. Results and discussion

The textural characteristics and surface chemistry of the adsorbents are very important for understanding the adsorption mechanism of an adsorbate. Table 1 shows the textural characteristics and pH_{PZC} of C3BRFBWM_PM, C3BRFBWM_SM and AC Darco.[16]

It can be seen from Table 1 that the MgO-templated materials are mainly mesoporous with a relatively high S_{BET} (~755 m^2 g^{-1}) and total pore and mesopore volume, although it should be noted that the mesopore volume of C3BRFBWM_SM is almost twice that of C3BRFBWM_PM. The commercial mesoporous activated carbon has a higher S_{BET} (*i.e.* 1857 m^2 g^{-1}) and V_T (*i.e.* 1.49 cm^3 g^{-1}), but a lower V_{meso} and thus, a lower V_{meso}/V_T ratio (*i.e.* 0.59). The BJH pore size distributions curves of the nanocarbons indicate a narrow pore size distribution (Fig. S1†). The mean mesopore size of C3BRFBWM_PM is 4.5 nm, while in the case of solution mixing it is 7 nm.[16] AC Darco have mesopores with different sizes and its BJH pore size distribution does not show any maximum. The surface chemistry of the three adsorbents is similar with pH_{PZC} values ranging from 2.4 to 3.6.

For the kinetic study, preliminary tests were carried out to evaluate the adsorption of the heavy metal. It was found that the adsorption of the heavy metal by the three adsorbents was negligible. The initial concentration (60 mg l^{-1} and 200 mg l^{-1} were tested) had no effect on the amount adsorbed by any of the three adsorbents. The pH of the solution (pH = 7) was higher than the pH_{PZC}, signifying that the surface was negatively charged. Therefore fewer protons were available to protonate functional groups on the surface of the adsorbents to form negatively charged sites. Hence the adsorption of a cation such as the heavy metal Cd^{2+} should have been favoured.[21,22] However the results obtained do not support this. The reason could be the low microporosity of the adsorbents which according to Alexandre-Franco *et al.*[10] is responsible for metal adsorption.

The SEM images show the morphological characteristics of the C3BRFBWM_PM nanocarbon (Fig. 2). The EDX spectra together with the quantitative analysis calculated from the peak area are also shown in Fig. 2. The material before adsorption is shown in Fig. 2a. The EDX spectrum confirms the presence of carbon and oxygen. After the adsorption of Cd^{2+} (Fig. 2b) the morphology of the material is similar and the composition does not indicate the presence of Cd^{2+}. The heavy metal Cd^{2+}, whose adsorption should have been favoured in the experimental conditions used, was not adsorbed on these materials. As can be seen in Fig. 1 the reactive dye contains Na, Cl and S. The EDX spectrum and quantitative analysis also reveals the presence of these elements in the adsorbent after contact with the dye (Fig. 2c) which were not present in the nanocarbon material before its use as adsorbent (Fig. 2a). On the other hand, after the adsorption of the dye + metal solution the EDX spectrum of the adsorbent indicates the presence of Cl, S and Cd (Fig. 2d). It can be seen that the Na atom has been replaced by the Cd atom, which supports the hypothesis of ion-exchange. No Na atoms are observed in the EDX spectrum after the adsorption of the dye + Cd^{2+} solution. It can be inferred therefore that Cd^{2+} is adsorbed by the adsorbents only in the presence of the dye due to an ion exchange between the Na^+ from the dye and the Cd^{2+}.

3.1. Effect of initial pH

The pH of an aqueous solution is an important parameter that affects the adsorption process due to the effect of electrostatic forces. The effect of pH on the removal of the dye (Fig. 3) was studied in the range between 2 and 12. When the pH was increased from 2 to 3 for the nanocarbons and to 4 for the activated carbon, the removal of dye decreased (from 51 to 39% for C3BRFBWM_PM; from 69 to 52% for C3BRFBWM_SM and from 95 to 65% for AC Darco). A further increase in pH up to 9 ensured that the extent of removal remained almost constant, whereas adsorption decreased as the pH increased from 9 to 12. At pH 2 there was a significantly high electrostatic attraction between the protonated surface groups of the carbon and

Table 1 Textural characteristics and pH_{PZC} of C3BRFBWM_PM and C3BRFBWM_SM as published by Acevedo *et al.*, 2014 and of AC Darco KB-KJ

Samples	S_{BET} (m^2 g^{-1})	V_T (cm^3 g^{-1})	V_{micro} (cm^3 g^{-1})	V_{meso} (cm^3 g^{-1})	V_{meso}/V_T	pH_{PZC}
C3BRFBWM_PM	762	0.85	0.27	0.58	0.68	3.6
C3BRFBWM_SM	752	1.35	0.27	1.08	0.80	3.3
AC Darco	1857	1.49	0.61	0.88	0.59	2.4

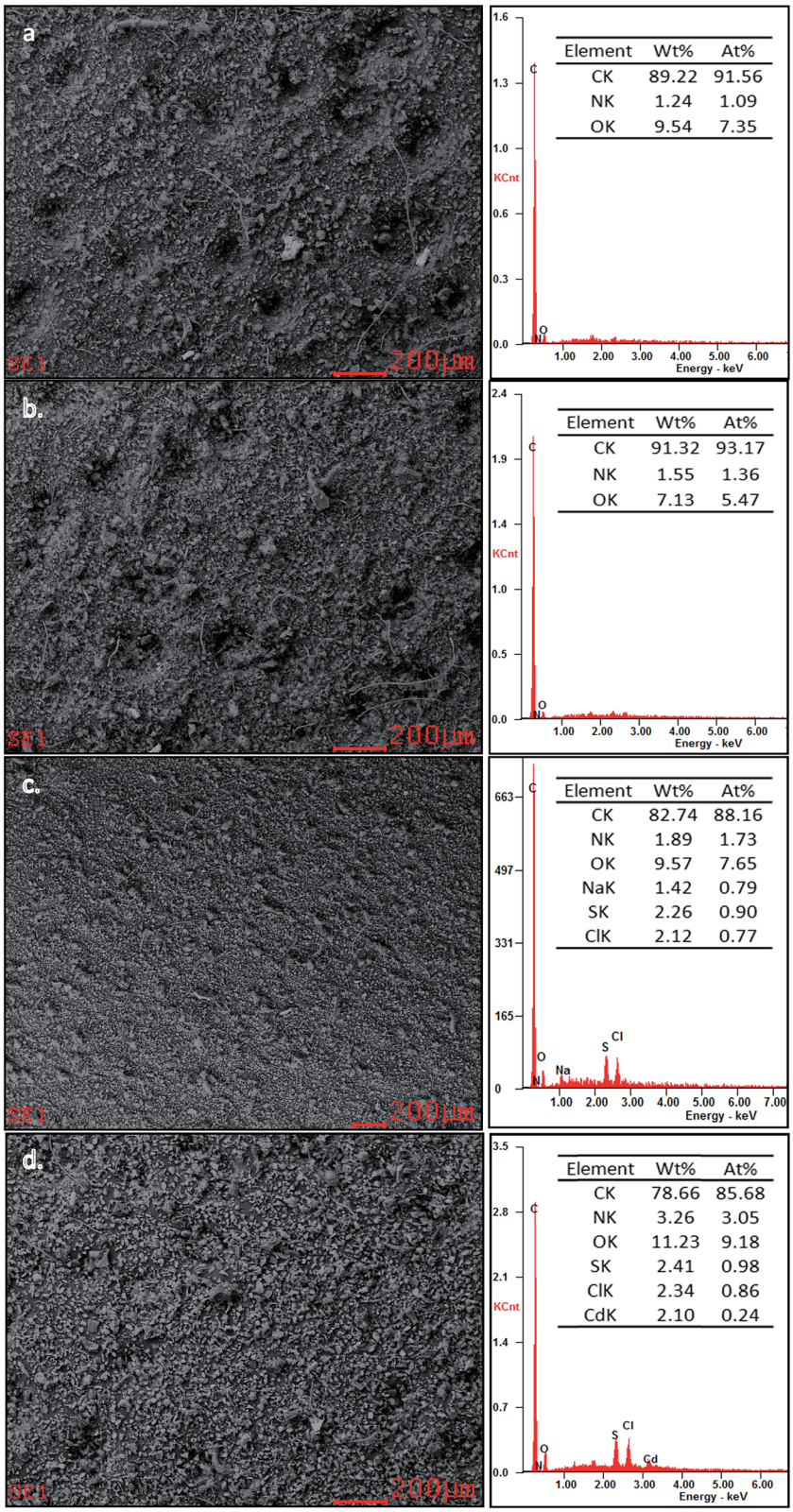

Fig. 2 SEM-EDX results. (a) Before adsorption, (b) after the adsorption of Cd^{2+}, (c) after the adsorption of dye and (d) after the adsorption of dye + Cd^{2+}.

anionic dye. As the pH of the solution increased, the number of negatively charged sites also increased which impeded the adsorption of dye anions due to electrostatic repulsion, while the number of positively charged sites decreased. Moreover, the presence of excess OH^- ions competing with the dye anions for the adsorption sites caused a decrease in the adsorption of dye

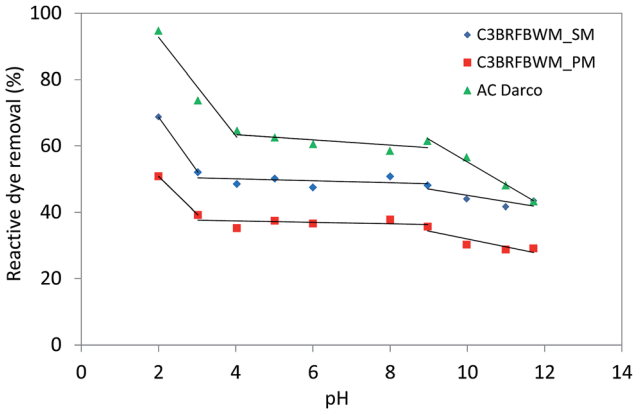

Fig. 3 Evolution of reactive dye removal as a function of pH.

at alkaline pH. However, in spite of the fact that the removal of dye decreased at alkaline pH, the adsorption of reactive dye was still quite high. This could be assigned to chemisorption, hydrogen bonding or hydrophobic interactions.[23,24]

A similar behaviour was observed for the adsorption of Congo Red,[25] Indigo Carmine dye,[26] Acid Blue 113 [27] and Rifafix Red 3BN.[28] The adsorbents studied had similar pH_{PZC} values. Thus the effect of pH on adsorption was similar in all three cases. The differences in the dye removal observed in Fig. 3 must therefore have been due to differences in their pore size distribution and S_{BET}.

The variation in the percentage of reactive dye and Cd^{2+} removal from the dye–metal mixture solution with the pH is shown in Fig. 4. It should be noted that the pH is below the onset of the hydrolysis of Cd^{2+} in order to prevent the precipitation of the metal.[29] Dye removal decreased when the pH increased from 2 to 4 for all the adsorbents, from 43 to 39% for C3BRFBWM_PM; from 62 to 56% for C3BRFBWM_SM and from 84 to 74% for AC Darco. Further increases in pH produced only slight decreases in dye removal up to pH 8. Although Cd^{2+} removal increased considerably between pH 2 and 3, further increases in pH produced only a gradual increase in Cd^{2+} removal.

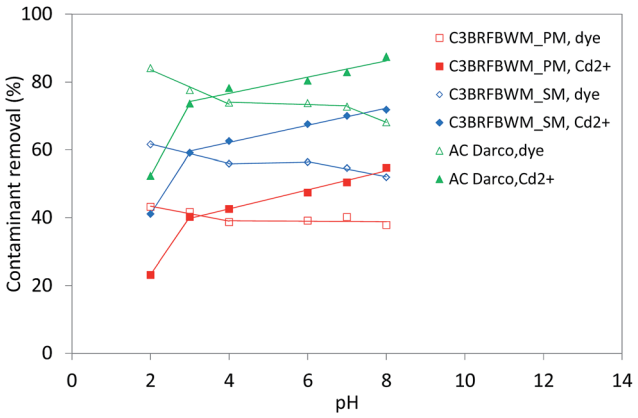

Fig. 4 Variation in reactive dye + Cd^{2+} removal as a function of pH.

Two factors need to be considered in order to explain the adsorption results: (1) the carbon surface charges which are responsible for electrostatic attraction/repulsion between the surface and the adsorbate and, (2) the ion exchange between the Na^+ from the dye and the Cd^{2+}. When the pH solution < pH_{PZC}, the carbon surface is mainly charged positively and the adsorption of anionic compounds such as the reactive dye, will be strongly favoured. It is for this reason that the electrostatic interaction of Cd^{2+} with the dye anion decreases. In addition, almost none of the Cd^{2+} was adsorbed onto the carbons due to the fact that the negative surface charges were smaller than the positive ones. Consequently, the percentage of metal removal was at its lowest value. However, the presence of the heavy metal cation in the solution gave rise to smaller dye removals at pH 2 in the case of the simultaneous adsorption (Fig. 4) compared to the dye solution (Fig. 3).

If solution pH > pH_{PZC}, the carbon surface will be charged negatively, favouring the adsorption of cationic compounds. As mentioned above, the adsorption of reactive dye was still quite high because of chemisorption, hydrogen bonding or hydrophobic interactions. Heavy metal was removed not only because of ion exchange between Na^+ from the dye and Cd^{2+}, but also because of the slight adsorption of Cd^{2+} on the negative charges of the carbon surface.

3.2. Adsorption isotherm of reactive dye

Equilibrium adsorption isotherms were used to determine the maximum adsorption capacities of the adsorbents. Adsorption isotherm models describe the manner in which the molecules of an adsorbate interact with the surface of the adsorbent. Equilibrium isotherms of dye adsorption (Fig. 5) were performed at pH 7 using initial dye concentrations in the range between 36 and 900 mg g^{-1} to be able to compare the adsorption capacities of the three adsorbents.

AC Darco was the material which adsorbed the highest amount of reactive dye per gram of adsorbent (527 mg g^{-1}). Nanocarbons showed a lower value of maximum adsorption capacity (~300 mg g^{-1}), which is higher than other maximum adsorption capacities for reactive Cibacron Brilliant Yellow 3G-P

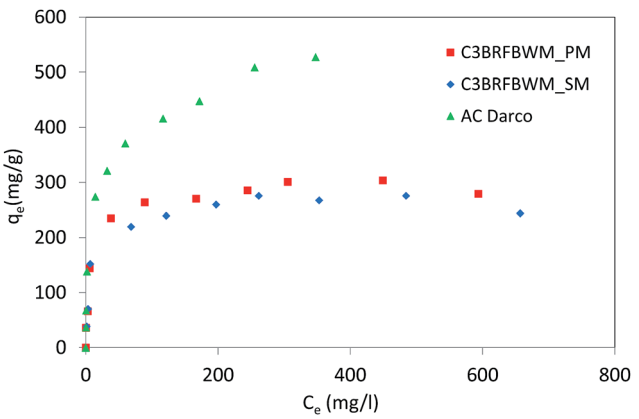

Fig. 5 Adsorption isotherms for Cibacron Brilliant Yellow 3G-P dye by C3BRFBWM_PM, C3BRFBWM_SM and Darco KB-KJ.

found in literature (*i.e.* 64.1 mg g^{-1} in the case of modified bentonite[30] or 209.51 mg g^{-1} for activated carbon[31]). The main advantage these mesoporous nanocarbons is the possibility of reusing waste materials in an efficient manner.

For the adsorption of the dye, the large S_{BET} and wide pore size distribution must have been determinant, since these are the textural characteristics that distinguish the AC Darco adsorbent from the nanocarbons. The volume of mesopores and narrow mesopore size where large dye molecules can be adsorbed, was not a relevant characteristic here since the maximum adsorption capacity of C3BRFBWM_SM was the same as that of C3BRFBWM_PM, although their mesopore volumes differed considerably: 1.08 and 0.58 cm^3 g^{-1} (Table 1) as did their mesopore size (7 and 4.5 nm, respectively). Surface chemistry is also important since AC Darco shows the highest adsorption capacity and the lowest pH_{PZC}. However its influence must have been lower than that of the textural characteristics because the differences in pH_{PZC} are smaller than those of texture.

The Langmuir, Freundlich and Langmuir–Freundlich models, well-known isotherm equations, were applied to obtain a deeper understanding of the adsorption data. The Langmuir model assumes that adsorption occurs in a monolayer where the active sites are identical and energetically equivalent.[32] Eqn (2) represents this isotherm where q_e and C_e are the dye uptake (mg g^{-1}) and concentration (mg l^{-1}) at equilibrium, q_{max} is the maximum adsorption capacity (mg g^{-1}) and b (l g^{-1}) represents the Langmuir equilibrium constant, respectively.

$$q_e = \frac{q_{max} b C_e}{1 + b C_e} \quad (2)$$

The Freundlich model (eqn (3)) is an empirical expression used to describe a heterogeneous system. It also describes reversible adsorption and is not restricted to the formation of monolayers.[33] The parameters of this equation are K_f, the Freundlich constant (mg^{1-n} l^n g^{-1}) and $1/n$, the heterogeneity factor of the Freundlich model which characterizes this heterogeneous system.

$$q_e = K_f C_e^{1/n} \quad (3)$$

The Langmuir–Freundlich model was formulated by Sips,[34,35] Crickmore and Wojciechowski[36] and, Bering and Serpinsky.[37] At low adsorbate concentrations, the model reduces to the Freundlich isotherm while, at higher concentrations, it predicts the monolayer adsorption capacity characteristic of the Langmuir isotherm (eqn (4)).

$$q_e = \frac{q_s a_s C_e^{n_s}}{1 + a_s C_e^{n_s}} \quad (4)$$

where q_s is the maximum adsorption capacity (mg g^{-1}), a_s, is a constant similar to the Langmuir constant and n_s represents the heterogeneity of the system.

The experimental data were adjusted to the isotherm models and the best fit was determined using a non-linear regression approach. Table 2 shows the parameters and statistical criteria used to identify the best isotherm equation for modelling the adsorption data. The targeted values were the correlation coefficient (r^2), the objective function value (F_{obj}, eqn (5)) and the mean absolute percentage deviation between the calculated ($q_{i,calc}$) and the experimental ($q_{i,exp}$) adsorption data, taking into account the number of experimental data (n_{dat}) (E_{abs}, eqn (6)).

$$F_{obj} = \sum_{i=1}^{n_{dat}} \left(\frac{q_{i,exp} - q_{i,calc}}{q_{i,exp}} \right)^2 \quad (5)$$

$$E_{abs} = \frac{100}{n_{dat}} \sum_{i=1}^{n_{dat}} \left| \frac{q_{i,exp} - q_{i,calc}}{q_{i,exp}} \right| \quad (6)$$

The adsorption of dye on the nanocarbons followed the Langmuir isotherm, which yielded similar q_{max} values in both cases (293.23 mg g^{-1} for C3BRFBWM_PM and 268.96 mg g^{-1} for C3BRFBWM_SM). The adjusted values of b are larger than for the commercial AC indicating a stronger bonding of the CBY dye to the nanocarbons. It is true that the Langmuir–Freundlich model also adjusted well to the data since the n_s values were close to 1 (0.810 for C3BRFBWM_PM and 0.835 for C3BRFBWM_SM). However, the best fit for the commercial activated carbon was obtained using the Langmuir–Freundlich model. Its n_s value was 0.464, while its q_s value was 745.48 mg g^{-1}, *i.e.* higher than the q_{max} produced by the Langmuir model (495.476 mg g^{-1}).

3.3. Adsorption study of the binary dye–heavy metal solution

The adsorption of heavy metal was very low. However, it was observed (Fig. 2d) that adsorption improved when dye was also in the solution. As explained above, an ion-exchange took place

Table 2 Parameters for the data modeling of dye adsorption isotherms on mesoporous nanocarbons and commercial activated carbon using different models

	C3BRFBWM_PM	C3BRFBWM_SM	AC Darco
Langmuir			
q_{max} (mg g^{-1})	293.23	268.96	495.48
b (l g^{-1})	0.132	0.134	0.079
r^2	0.973	0.968	0.936
F_{obj}	0.705	1.640	0.528
E_{abs}	14.011	24.548	12.691
Freundlich			
K_f (mg^{1-n} l^n g^{-1})	95.86	75.80	120.17
$1/n$	0.193	0.224	0.260
r^2	0.875	0.894	0.975
F_{obj}	0.109	1.654	0.180
E_{abs}	8.326	25.458	9.844
Langmuir–Freundlich			
q_s (mg g^{-1})	304.48	279.30	745.48
a_s (l mg^{-1})^{n_s}	0.174	0.158	0.151
n_s	0.810	0.835	0.464
r^2	0.972	0.964	0.992
F_{obj}	1.358	1.979	0.284
E_{abs}	24.887	21.802	9.392

between the Cd^{2+} and the exchangeable cation (Na^{+}) from the dye. A multicomponent solution can exhibit three possible types of adsorption effects under competitive conditions: synergism, antagonism or non-interaction.[5] The same behaviour was observed for the three adsorbents used in the present research work. The removal of the dye and heavy metal increased when the two components were present in the solution (Fig. 6). Therefore the binary solution must have experienced synergistic adsorption effects. It should also be noted that the binary solution must favour the adsorption of Cd^{2+} since the increase in dye removal is lower than that of the metal. AC Darco experienced the highest synergic effect, with the removal of Cd^{2+} increasing by 72.11%. This adsorbent also achieved the highest metal and dye removal from the binary solution, 85.40 and 69.36% respectively.

At pH 7 (*i.e.* $pH_{PZC} < pH_{solution}$), the surface carbon groups were negatively charged. The dye was adsorbed by chemisorption, hydrogen bonding or hydrophobic interactions, the heavy metal ions by electrostatic forces and, in the case of the binary CBY–Cd^{2+} solution, an ion exchange between Na^{+} and Cd^{2+} occurred that yielded a positive electronic density because of the difference between the two interchangeable ions which favoured the adsorption of CBY–Cd^{2+} on the negatively charged surface of the carbons.

Fig. 7 shows the adsorption isotherms corresponding to the reactive dye (Fig. 7a) and the Cd^{2+} (Fig. 7b) of the dye–metal mixture solution for the three adsorbents. Both the dye adsorption isotherm and the metal adsorption isotherm showed higher maximum adsorption capacities when AC Darco was used, (*i.e.* $q_{max} = 606$ mg g^{-1} for dye adsorption and 53 mg g^{-1} for metal). The maximum adsorption capacity values corresponding to the nanocarbons in the adsorption of the dye and metal of the binary solution were higher than in the individual solutions ($q_{max,dye} = 322$ mg g^{-1}, $q_{max,Cd^{2+}} = 37$ mg g^{-1} for C3BRFBWM_PM and $q_{max,dye} = 456$ mg g^{-1} and $q_{max,Cd^{2+}} = 37$ mg g^{-1} for C3BRFBWM_SM) although the adsorption capacity was lower than that achieved with AC Darco. The differences observed in the values of the maximum adsorption capacity of the nanocarbons and the commercial AC are mainly assigned to the porous textures of the three materials used as adsorbents (Table 1) even though their surface chemistries as quantified by means of the pH_{PZC} value are not very different (*i.e.* all three values are between 2.4 and 3.6, the lowest that corresponding to the commercial AC). In addition, at pH = 7 the three adsorbents have negative charges and the dye is an anion. On the other hand the BET surface area of the commercial AC is more than double of that of the nanocarbons (1857 *vs.* 752 and 762 m^2 g^{-1}). In addition the pore size distribution is also different. The micropore volume of the commercial AC is more than double that of the nanocarbons prepared and the total pore volume is also higher. The mesopore volume value however, lies between those of the two nanocarbons. The results

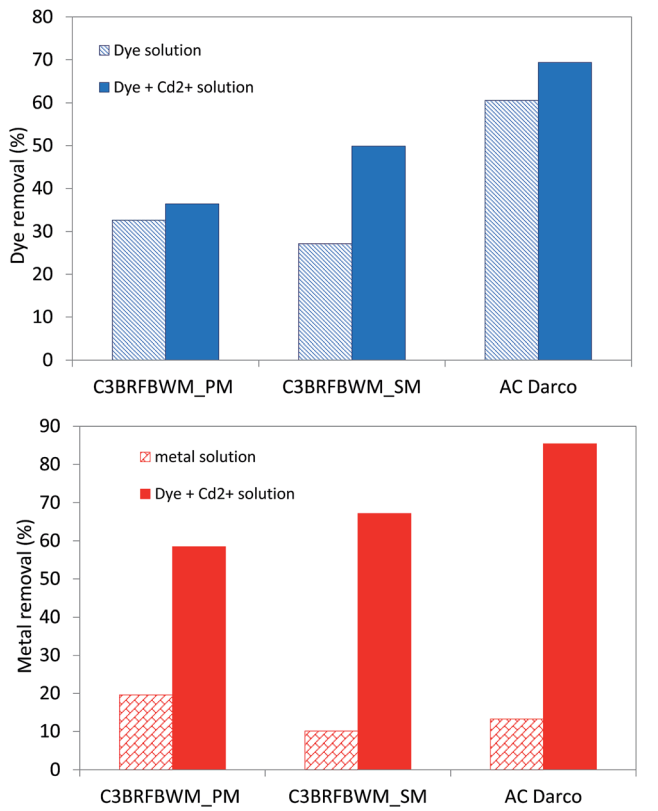

Fig. 6 Results of the multicomponent adsorption in the binary mixtures dye + Cd^{2+} with an initial concentration of 900 mg l^{-1} for dye and 60 mg l^{-1} Cd^{2+} at pH 7.

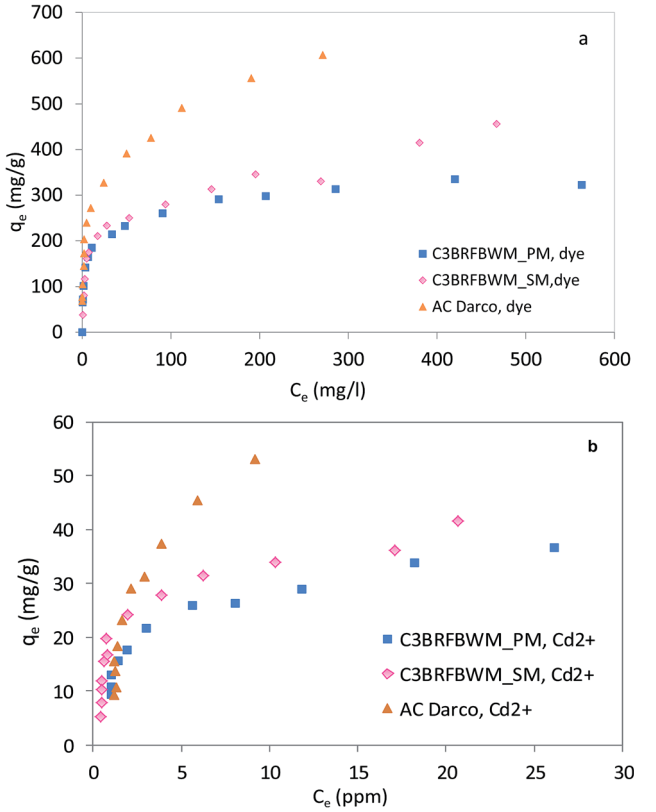

Fig. 7 Adsorption isotherms of reactive dye (a) and Cd^{2+} (b) of the mixture dye + Cd^{2+} solution on C3BRFBWM_PM, C3BRFBWM_SM and Darco KB-KJ.

obtained in the present research work indicate that a higher mesopore pore volume was not decisive in this case.

In the literature the values of maximum adsorption capacity for reactive CBY dye adsorption were lower.[32,33,38] For the adsorption of Cd^{2+} the values ranged between 14.33 mg g^{-1} on polyaniline grafted chitosan[39] and 61.35 mg g^{-1} on hazelnut husk AC.[40]

As observed in the case of the adsorption of the dye (Fig. 5), the most important parameters were the S_{BET} and pore size distribution. The same applies to Cd^{2+} although in the binary system, the adsorption of the metal cation is linked to that of the dye because of the ion exchange with Na^{+}. However, the adsorption of dye and metal from the binary solution must also have been affected by the higher total and mesopore volume for the same S_{BET} and V_{micro}, since the maximum adsorption capacities of C3BRFBWM_SM were higher than those of C3BRFBWM_PM.

4. Conclusions

The commercial AC had a higher S_{BET}, total pore volume, micropore volume and wide pore size distribution and a lower pH_{PZC} than the nanocarbons.

The adsorption of Cd^{2+} was poor in all three materials tested, unlike the adsorption of dye which was successfully achieved. Increasing the pH from 2 to 3–4 caused a reduction in adsorption capacity due to a decrease in the electrostatic interactions between the carbon surface and the anionic dye. Further increases of up to 9 did not produce any variations in dye removal. In the case of the heavy metal, a rise in the pH from 2 to 3 had a beneficial effect. Further increases led to a greater removal of Cd^{2+}.

Synergism appeared and the removal of both contaminants increased when the two components were present in the solution together, especially in the case of the heavy metal. A higher total pore volume, mesopore volume, S_{BET} and different pore size distribution all played a determinant role in the adsorption of both contaminants in the binary solution.

Acknowledgements

The research leading to these results has received funding from the Spanish MICINN CTM2009-10227. BA thanks the Government of the Principado the Asturias for the award of a predoctoral grant with funds from the PCTI Asturias.

References

1 Y. Al-degs, M. A. M. Khraisheh, S. J. Allen and M. N. Ahmad, *Water Res.*, 2000, **34**, 927–935.
2 L. D. T. Prola, E. Acayanka, E. C. Lima, C. S. Umpierres, J. C. P. Vaghetti, W. O. Santos, S. Laminsi and P. Djifon, *Ind. Crops Prod.*, 2013, **46**, 328–340.
3 N. F. Cardoso, E. C. Lima, I. S. Pinto, C. V. Amavisca, B. Royer, R. B. Pinto, W. S. Alencar and S. F. P. Pereira, *J. Environ. Manage.*, 2011, **92**, 1237–1247.
4 N. Willmott, J. Guthrie and G. Nelson, *J. Soc. Dyers Colour.*, 1998, **114**, 38–41.
5 V. Hernández-Montoya, M. A. Pérez-Cruz, D. I. Mendoza-Castillo, M. R. Moreno-Virgen and A. Bonilla-Petriciolet, *J. Environ. Manage.*, 2013, **116**, 213–221.
6 X. Liu and D.-J. Lee, *Bioresour. Technol.*, 2013, **160**, 24–31.
7 Y. S. Ho and G. McKay, *Water Res.*, 2000, **34**, 735–742.
8 P. A. Cox, *The Elements on Earth*, Oxford University Press, Oxford, 1995.
9 J. H. Mennear, *Cadmium Toxicity*, Marcel Dekker, New York, 1979.
10 M. Alexandre-Franco, C. Fernández-González, M. Alfaro-Domínguez and V. Gómez-Serrano, *J. Environ. Manage.*, 2011, **92**, 2193–2200.
11 S. D. Khattri and M. K. Singh, *Environ. Prog. Sustainable Energy*, 2012, **31**, 435–442.
12 D. Sun, X. Zhang, Y. Wu and X. Liu, *J. Hazard. Mater.*, 2010, **181**, 335–342.
13 G. Crini, *Bioresour. Technol.*, 2006, **97**, 1061–1085.
14 B. Acevedo, C. Barriocanal, I. Lupul and G. Gryglewicz, *Fuel*, 2015, **151**, 83–90.
15 T. Morishita, T. Tsumura, M. Toyoda, J. Przepiórski, A. W. Morawski, H. Konno and M. Inagaki, *Carbon*, 2010, **48**, 2690–2707.
16 B. Acevedo and C. Barriocanal, *Microporous Mesoporous Mater.*, 2015, **209**, 30–37.
17 Y. S. Wang, C. Y. Wang and M. M. Chen, *New Carbon Mater.*, 2010, **24**, 187–190.
18 M. Inagaki, H. Orikasa and T. Morishita, *RSC Adv.*, 2011, **1**, 1620–1640.
19 B. Acevedo, C. Barriocanal and R. Álvarez, *Fuel*, 2013, **113**, 817–825.
20 C. Moreno-Castilla, M. V. Lopez-Ramon and F. Carrasco-Marin, *Carbon*, 2000, **38**, 1995–2001.
21 V. K. Gupta, S. A. Nayak, S. Agarwal, M. Chaudhary and I. Tyagi, *J. Mol. Liq.*, 2014, **190**, 215–222.
22 C. Troca-Torrado, M. Alexandre-Franco, C. Fernandez-Gonzalez, M. Alfaro-Dominguez and V. Gomez-Serrano, *Fuel Process. Technol.*, 2011, **92**, 206–212.
23 G. Newcombe and M. Drikas, *Carbon*, 1997, **35**, 1239–1250.
24 G. Newcombe, C. Donati, M. Drikas and R. Hayes, *Water Supply*, 1996, **14**, 129–144.
25 C. Namasivayam and D. Kavitha, *Dyes Pigm.*, 2002, **54**, 47–58.
26 U. R. Lakshmi, V. C. Srivastava, I. D. Mall and D. H. Lataye, *J. Environ. Manage.*, 2009, **90**, 710–720.
27 V. K. Gupta, B. Gupta, A. Rastogi, S. Agarwal and A. Nayak, *J. Hazard. Mater.*, 2011, **186**, 891–901.
28 J. J. M. Órfão, A. I. M. Silva, J. C. V. Pereira, S. A. Barata, I. M. Fonseca, P. C. C. Faria and M. F. R. Pereira, *J. Colloid Interface Sci.*, 2006, **296**, 480–489.
29 J. E. Fergusson, *The Heavy Elements: Chemistry, Environmental Impact and Health Effects*, Pergamon Press, Oxford, 1990.
30 Q. Hu, Z. Xu, S. Qiao, F. Haghseresht, M. Wilson and G. Q. Lu, *J. Colloid Interface Sci.*, 2007, **308**, 191–199.
31 Y. S. Al-Degs, M. I. El-Barghouthi, A. H. El-Sheikh and G. M. Walker, *Dyes Pigm.*, 2008, **77**, 16–23.

32 I. Langmuir, *J. Am. Chem. Soc.*, 1918, **40**, 1361–1403.
33 H. Freundlich, *New conception in colloidal chemistry, colloid and capillary chemistry*, Methuen, Londres, 1926.
34 J. R. Sips, *J. Chem. Phys.*, 1948, **16**, 490–495.
35 J. R. Sips, *J. Chem. Phys.*, 1950, **18**, 1024–1026.
36 P. J. Crickmore and B. W. Wojciechowski, *J. Chem. Soc., Faraday Trans. 1*, 1977, **73**, 1216–1223.
37 B. P. Bering, V. V. Serpinskii and B. Acad, *Bull. Acad. Sci. USSR, Div. Chem. Sci.*, 1974, **23**, 2342–2353.
38 Z. Aksu, *Biochem. Eng. J.*, 2001, **7**, 79–84.
39 R. Karthik and S. Meenakshi, *Chem. Eng. J.*, 2015, **263**, 168–177.
40 M. Imamoglu, H. Yıldız, H. Altundag and Y. Turhan, *J. Dispersion Sci. Technol.*, 2015, **36**, 284–290.